Apatites in lunar KREEP basalts: The missing link to understanding the H isotope systematics of the Moon

Romain Tartèse[1]*, Mahesh Anand[1,2], Francis M. McCubbin[3], Stephen M. Elardo[3], Charles K. Shearer[3], and Ian A. Franchi[1]
[1]Planetary and Space Sciences, The Open University, Walton Hall, Milton Keynes MK7 6AA, UK
[2]Department of Earth Sciences, The Natural History Museum, Cromwell Road, London SW7 5BD, UK
[3]Institute of Meteoritics, University of New Mexico, 200 Yale Boulevard SE, Albuquerque, New Mexico 87131, USA

ABSTRACT

Recent re-analyses of lunar samples have undoubtedly measured indigenous water, challenging the paradigm of a "dry" Moon, and arguing that some portions of the lunar interior are as wet as some regions of the Earth's mantle and that water in both planetary bodies likely share a common origin. Mare basalts indirectly sample the lunar mantle and are affected by petrogenetic processes such as crystallization and degassing that can modify characteristics of indigenous water in primary mantle melts. Analyses of apatite in phosphorus-rich KREEP (K + REE [rare earth elements] + P) basalts may provide more reliable estimates for the water content of lunar magmas, as some apatites likely crystallized before substantial degassing occurred. In lunar KREEP basalt sample 15386, apatite H_2O content and H isotopic composition suggest that degassing occurred during apatite crystallization, the lowest δD value of 90‰ ± 100‰ representing an upper limit for the isotopic composition of water in the parental magma. Interpretation of the data for KREEP basalt 15386 suggests that this basalt is characterized by relatively elevated H_2O contents and CI chondrite–type δD values, similar to those proposed for other mare basalts and pyroclastic glasses. On the other hand, most of the apatites in lunar KREEP basalt 72275 and lunar meteorite NWA 773 crystallized before degassing and H isotope fractionation, and their D/H ratios thus directly reflect those of their source regions. These apatites have an average δD value of –130‰ ± 50‰, suggesting the presence of a water reservoir in the Moon characterized by moderate H_2O contents and H isotopic composition similar to that of Earth's interior. These findings imply that significant amounts of water in the Moon were inherited from the proto-Earth, surviving the purported Moon-forming impact event.

INTRODUCTION

It is now well established that indigenous H-bearing species (H, OH, and H_2O, referred to as the component "water" herein) are present in lunar volcanic glasses, in olivine-hosted melt inclusions within them (Hauri et al., 2011; Saal et al., 2008, 2013), in nominally anhydrous minerals from the lunar highlands (Hui et al., 2013), and in apatite in nearly all lunar lithologies (Barnes et al., 2013, 2014; Boyce et al., 2010; Greenwood et al., 2011; McCubbin et al., 2010a, 2010b, 2011; Tartèse et al., 2013). The isotopic composition of this water can provide clues regarding its origin. H isotope ratios in lunar apatites were first reported by Greenwood et al. (2011), who ascribed the elevated D/H ratios measured in most samples to a cometary origin. Subsequently, Tartèse and Anand (2013) proposed that indigenous lunar water could instead be characterized initially by CI chondrite–like D/H ratios, and the elevated D/H ratios measured in apatites from mare basalts being a result of fractionation of H and D during magmatic degassing of H_2. From analysis of CI chondrite–type D/H ratios in melt inclusions in lunar volcanic glasses, Saal et al. (2013) later came to the same conclusion, and H_2 degassing is now considered as the likely mechanism to account for elevated D/H ratios measured in water-rich lunar samples (Sharp et al., 2013; Tartèse et al., 2013). Finally, recent analyses carried out in apatites from the ca. 4.4 Ga Mg-suite norite samples 78235 and 77215, from the lunar highlands, yielded D/H ratios comparable to terrestrial values (δD of ~100‰ to – 300‰; Barnes et al., 2014). In this study, we investigated the water content and its H isotopic composition in apatites from KREEP (K + REE [rare earth elements] + P) basalts, which represent an important lunar rock type not previously investigated for their OH and D/H systematics. KREEP basalts can provide unique insights into the H isotopic composition of the Moon because they represent a mixture of different volatile reservoirs, the mare source region and the geochemical component KREEP, the latter dominating the volatile signature of the crust (McCubbin et al., 2011). Furthermore, elevated P_2O_5 contents in these samples compared to mare basalts (e.g., Taylor et al., 2012, and references therein) likely resulted in earlier saturation of apatite. Consequently, KREEP basalts are more likely to have crystallized apatite before substantial H degassing had occurred, which in turn would have resulted in apatites recording the H isotopic composition of the H source reservoir.

*E-mail: Romain.Tartese@open.ac.uk.

WATER CHARACTERISTICS OF APATITE IN KREEP BASALTS

A brief background, including key features and occurrence of KREEP basalts in Apollo Missions collections, along with their petrogenesis, is provided in the GSA Data Repository[1]. Electron probe microanalysis (EPMA) data were acquired for apatites in lunar KREEP basalts 15386, 15382, and 72275, and in lunar meteorite NWA 2977 (paired with meteorite NWA 773) (Table DR1 in the Data Repository). The volatile compositions of these apatites are reported in the truncated ternary F-Cl-OH diagram (Fig. 1A; assuming apatite X-site is completely filled with F, Cl, and OH only). EPMA data for apatites in KREEP basalts plot close to the F apex. For most of the analyses, the calculated OH contents are relatively low, and volatile compositions range between those of low-OH mare basalt apatite and low-Cl apatite from the lunar highlands (Fig. 1A).

Secondary ion mass spectrometry (SIMS) analyses of apatites in sample 72275 are characterized by large variations in OH contents, from ~90 ppm to 1600 ppm, with homogeneous δD values with a weighted average of –113‰ ± 62‰ (2σ, mean square weighted deviation [MSWD] = 1.08) (Fig. 1B; Table DR2). Apatites in meteorite NWA 773 have OH contents ranging from ~1000 ppm to 5400 ppm, and δD values between –273‰ ± 139‰ and 184‰ ± 140‰ (Fig. 1B; Table DR2). The values for NWA 773 are consistent with SIMS measurements of apatites in the paired meteorite NWA 2977 (OH ~1900–4700 ppm, average δD = –110‰ ± 30‰; McCubbin et al., 2010b; Wang et al., 2012). Finally, in lunar sample 15386, apatite OH contents range from ~200 ppm to 1500 ppm, with associated δD values displaying very large variations, from 89‰ ± 99‰ to 778‰ ± 123‰ (Fig. 1B; Table DR2). Interestingly, δD values measured in apatites in sample 15386 actually range from low δD values similar to those measured in apatites in KREEP samples 72275 and NWA 773 and in Mg-suite norites 78235 and 77215, up to δD values typical of those measured in apatites in mare basalts collected during the Apollo 15 mission. It is difficult to directly compare OH

[1]GSA Data Repository item 2014135, general description of KREEP basalts, and additional figures and tables with the results, is available online at www.geosociety.org/pubs/ft2014.htm, or on request from editing@geosociety.org or Documents Secretary, GSA, P.O. Box 9140, Boulder, CO 80301, USA.

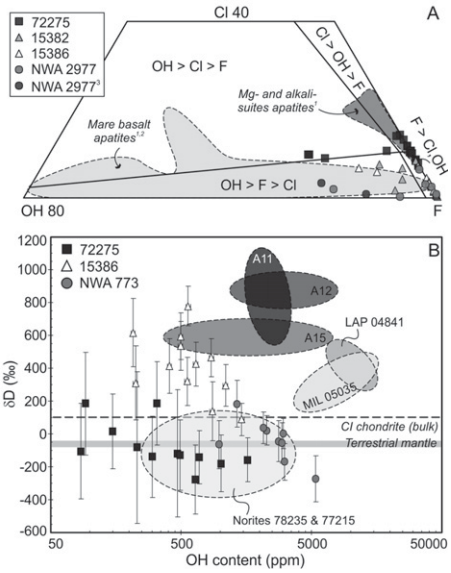

Figure 1. A: Truncated ternary plot of apatite X-site occupancy (mol%), assuming that X-site is completely filled with F, Cl, and OH, for lunar KREEP (K + REE [rare earth elements] + P) basalts 15386, 15382, 72275, and lunar meteorite NWA 2977 (paired with NWA 773). Fields for relative abundances of F, Cl, and OH in melts from which apatites crystallized are from McCubbin et al. (2013). References are: 1—McCubbin et al. (2011); 2—Tartèse et al. (2013); 3—McCubbin et al. (2010b). Two points for NWA 2977 apatites are ion probe data from McCubbin et al. (2010b). B: OH contents and δD values measured in apatites in KREEP basaltic samples 15386 and 72275, and meteorite NWA 773. Data for Apollo 11 (A11), Apollo 12 (A12), and Apollo 15 (A15) missions, and for basaltic meteorites LAP 04841 and MIL 05035, are from Tartèse et al. (2013); data for norites 78235 and 77215 are from Barnes et al. (2014). δD range for terrestrial mantle (–60‰ ± 20‰) is from Lécuyer et al. (1998), and value for bulk Cl chondrites is from Alexander et al. (2012).

contents measured by SIMS with those calculated from EPMA analyses, as most of the latter are below the detection limit of ~2700 ppm OH (McCubbin et al., 2010a). In samples 72275 and 15386, only 5 out of 31 EPMA OH contents are above this detection limit, which is consistent with measured OH contents in apatites lower than ~2700 ppm. In meteorite NWA 773, measured apatite OH contents are from ~1000 to 5400 ppm, consistent with EPMA OH contents that range from <2700 ppm to 6500 ppm.

APATITES IN SAMPLE 15386: A DIRECT RECORD OF MAGMATIC DEGASSING OF H_2

Analyses carried out in apatite grains in KREEP basalt 15386, and in some grains in meteorite NWA 773, display a trend of increasing δD values with decreasing OH contents (Fig. 1B), which could have resulted from late or post-crystallization inward diffusion of OH from an isotopically light reservoir of H (e.g., solar wind H in lunar regolith) or from degassing of H-bearing species from the magma during apatite crystallization. To investigate this issue, we examined the petrographic context of the analyzed apatite grains in sample 15386 to try and correlate analyses with the timing of crystallization. Many grains were within the matrix and it could not be determined whether they crystallized late or early on a textural basis alone (Fig. DR2). However, a few grains allowed some key observations to be made. One of the apatite grains, partially enclosed within a merrillite grain and in contact with late-stage quenched melt (i.e., glass), contains a melt inclusion (Figs. 2A and 2B). The distribution of ^{1}H shows that it is enriched in the trapped melt inclusion compared to the host apatite (Fig. 2C), indicating that H is indeed incompatible in apatite (Vander Kaaden et al., 2012) (matrix effects between the different phases are considered negligible compared to the actual variations in H abundance). Furthermore, H is even more enriched in the quenched glass next to the apatite-merrillite assemblage, illustrating extreme H enrichments in the very last melt fractions (Fig. 2C). In contrast, F is concentrated in the apatite, exemplifying its strong compatible behavior into apatite (Fig. 2C) (Vander Kaaden et al., 2012). Finally, profiles of ^{1}H and ^{19}F variations show that boundaries between the apatite and the adjacent glass and melt inclusion are characterized by sharp changes in H and F contents over a distance of ~1–2 µm (Fig. 2C; Fig. DR3), which seems to preclude significant diffusive exchange and re-equilibration between these different phases, as typical length scales for OH mobility in terrestrial apatites are several tens of microns (Boyce and Hervig, 2008).

In contrast to most of the apatite grains in sample 15386, closely associated with late-stage mesostasis areas, we observed an apatite grain (Ap5) included within a pyroxene, suggesting a relatively early crystallization (Fig. DR2). Interestingly, this grain is characterized by a low δD and high OH content. This is the opposite of what would be expected during contamination by an isotopically light source of H; however it is exactly what one would expect if the observed OH-δD relationship resulted from crystallization during magmatic degassing of H_2. Indeed, an increase of the D/H ratios with decreasing water contents can result from degassing of H_2 from the crystallizing magmas, the light isotope H being preferentially lost to space compared to D (for discussion of additional complexities such as possible kinetics effects or nonlinear degassing, see Sharp et al., 2013; Tartèse and Anand, 2013; Tartèse et al., 2013). The H isotope fractionation during volatile loss into a vacuum is given by $\sqrt{M1/M2}$, where M1 and M2 are the masses of the volatile phase isotopologues (e.g., Esat, 1988), here H_2 (molecular mass of 2) and HD (molecular mass of 3). The change in the isotopic composition of H during H_2 loss by Rayleigh fractionation follows the relationship $R = R_0 \times f^{(\alpha-1)}$, where R_0 and R are the initial and final D/H ratios in the magma for a fraction f of remaining hydrogen. Starting from the most OH-rich apatite analysis (and excluding analysis Ap14#1), the OH-δD values measured in apatites in sample 15386 can be fitted with a power law relationship characterized by a power law exponent of –0.220 ± 0.074, corresponding to an α value of 0.780 ± 0.074, which is in excellent agreement with the theoretical α value of 0.816 associated with H_2 degassing. Results from modeling the evolution of H_2O content and δD of a melt undergoing degassing of H_2, starting from the high-OH values measured in meteorite NWA 773 and two initial δD values of –100‰ and 100‰, encompasses the range of OH-δD characteristics measured in most of the apatites in NWA 773 and 15386, and suggest

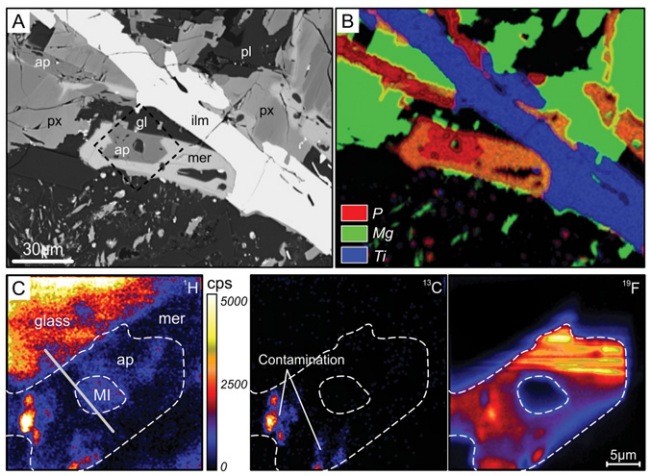

Figure 2. A: Back-scattered electron image of area enclosing a glass + melt inclusion + apatite assemblage in lunar sample 15386 ap—apatite; gl—glass; ilm—ilmenite; mer—merrillite; pl—plagioclase; px— pyroxene. B: Corresponding combined X-ray map including P, Mg, and Ti. C: Secondary ion images showing distribution of ^{1}H, ^{13}C, and ^{19}F in an apatite and the melt inclusion (MI) it hosts (cps—counts per second). Corresponding area is depicted in A by dashed black square. Thick gray line displayed on ^{1}H map indicates location of profile shown in Figure DR3 (see footnote 1).

apatite crystallization during up to 80%–90% H_2 degassing (Fig. 3).

IMPLICATIONS FOR WATER IN THE LUNAR INTERIOR

The amount of H_2O dissolved in the melt when apatite crystallized can be estimated from

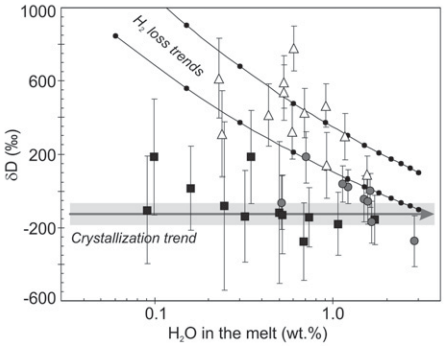

Figure 3. Proposed geochemical model, combining crystallization of nominally anhydrous minerals and magmatic degassing of H_2, to account for measured OH contents and D/H ratios in apatites from lunar KREEP (K + REE [rare earth elements] + P) basalts. Symbols are same as in Figure 1B.

the measured OH contents in apatite grains. Unfortunately, appropriate partition coefficients are not well constrained for typical lunar basalt compositions and conditions (pressure, temperature, oxygen fugacity) under which these magmas crystallized. Two studies have determined the apatite-melt partitioning behavior of F, Cl, and OH in terrestrial and martian basaltic systems (Mathez and Webster, 2005; Vander Kaaden et al., 2012), the latter representing the best lunar analogue for present purposes. Partition coefficients for H_2O between apatite and melt ($D_{H_2O}^{apatite/melt}$) determined by Vander Kaaden et al. (2012) ranges from 0.05 to 0.3. For ternary compositions of apatite similar to those measured in KREEP basalts 72275 and 15386, with relatively low water contents, a $D_{H_2O}^{apatite/melt}$ value of ~0.05 is most appropriate. For apatites in meteorite NWA 773, water contents are slightly higher, and Vander Kaaden et al. (2012) indicated that a $D_{H_2O}^{apatite/melt}$ value of ~0.10 is more applicable. Importantly, these D values only apply to equilibrium crystallization conditions. Using these partition coefficients, estimates for H_2O contents in the KREEP basalt melts at the time of apatite crystallization ranged between ~0.1 and 1.7 wt% for lunar sample 72275, ~0.2 and 1.5 wt% for sample 15386, and ~0.5 and 2.8 wt% for NWA 773 (Fig. 3). In basalt 72275, apatite grains are characterized by large OH variations at relatively constant D/H ratios, reflecting protracted crystallization only (Tartèse et al., 2013). In contrast, OH-δD characteristics of apatites in basalt 15386 reflect crystallization during degassing of H_2. In non-KREEP mare basalts, phosphate saturation occurs very late, probably after more than 96% crystallization (e.g., Sha, 2000; Tartèse and Anand, 2013). KREEP basalts are enriched in P (e.g., Taylor et al., 2012), so it is likely that phosphate saturation occurs earlier, after around 85%–90% crystallization (Harrison and Watson, 1984). Assuming that the lowest-OH-content apatite in sample 72275 crystallized after 85%–90% crystallization yields an initial H_2O content of 99–144 ppm in the parental melt. For sample 15386, the first apatite to crystallize is the wettest one, considering the degassing scenario detailed above. Assuming that it also crystallized after 85%–90% crystallization yields an initial H_2O content of ~1690–2460 ppm in the parental melt. Finally, it seems that a few apatites in meteorite NWA 773 with low δD values crystallized before degassing. Considering that the low-H_2O apatite with a low δD value of ~–100‰ formed after 85%–90% crystallization yields an initial H_2O content of ~560–820 ppm in the parental melt, intermediate between samples 72275 and 15386. If these basalts formed by 5%–15% partial melting, their mantle source regions would have contained ~6–23 ppm H_2O for lunar basalt 72275, ~100–390 ppm H_2O for basalt 15386, and ~34–130 ppm H_2O for meteorite NWA 773. These estimates overlap with recent estimates of H_2O contents for non-KREEP mare basalt source regions (Tartèse et al., 2013) and high-Ti volcanic glass source regions (Hauri et al., 2011), all of them being consistent with the range of ~50–250 ppm H_2O estimated for the terrestrial upper mantle (e.g., Saal et al., 2002). However, all these estimates for lunar basalts should be taken with caution until we gain better constraints on the partitioning behavior of F, Cl, and OH into apatites crystallizing from lunar magmas. Finally, if KREEP basalts formed by less than 5% partial melting, estimates for H_2O contents of the mantle source regions would be lower than values reported above.

The data reported in this study suggest that KREEP basalts provide reliable estimates for the water content of lunar magmas based on apatite analyses because at least some of them seem to have crystallized before substantial degassing of H occurred. The H record in apatite prior to substantial degassing is also important for constraining the H isotopic composition of the KREEP basalt source regions. In KREEP basalt 15386, the lowest δD value of 98‰ ± 99‰ represents an upper limit for the initial δD as the magma might have already started to degas before the onset of apatite crystallization. In any case, such a δD value of ~100‰ is consistent with pre-degassing δD values estimated for non-KREEP mare basalts (Tartèse et al., 2013) and for high-Ti pyroclastic magmas (Saal et al., 2013). KREEP basalt 15386, other typical mare basalts, and high-Ti pyroclastic glasses seem to be characterized by elevated H_2O contents and CI chondrite–type δD values (Fig. 1B), which might indicate a close genetic relationship between them. On the other hand, nearly all apatites in KREEP basalt 72275 and some apatites in lunar meteorite NWA 773 have not been affected by extensive degassing processes. Therefore, measured δD values in those grains are likely to be closer to the D/H ratios of their lithologic source regions. These apatites are characterized by an average δD value of ~–130‰ ± 50‰, which is strikingly similar to the average δD value of apatites from Mg-suite norite 78235 (Barnes et al., 2014) (Fig. 1B). Such observations strongly imply the presence of a water reservoir in the lunar interior characterized by a moderate H_2O content and a low δD value, slightly lower than the present-day terrestrial mantle (δD = –60‰ ± 20‰; Lécuyer et al., 1998). However, the δD value of the proto-Earth mantle could have been lower by ~100‰–200‰ compared to its present-day value (e.g., Sharp et al., 2013), having δD values of ~–200‰ ± 50‰, which would be consistent with this low-δD lunar reservoir. The most straightforward explanation for such similarities would be for water sampled from this lunar reservoir to be directly inherited from the proto-Earth mantle material, which survived the impact origin of the Moon. We caution against any over-interpretation of the limited data set at this stage, and further data are needed to confirm this hypothesis.

APPENDIX. ANALYTICAL TECHNIQUES

Electron Probe Microanalysis (EPMA)

Major element compositions of apatite grains in KREEP basalt samples were analyzed using a JEOL JXA 8200 electron microprobe (Institute of Meteoritics at the University of New Mexico, USA), following the apatite EPMA procedure outlined by McCubbin et al. (2010a, 2011). Results are given in Table DR1 (see footnote 1).

Secondary Ion Mass Spectrometry (SIMS)

OH contents and H isotope compositions were measured in apatite grains using the Cameca NanoSIMS 50L at the Open University (UK), using the protocol detailed by Barnes et al. (2013) and Tartèse et al. (2013), and apatite standards described by McCubbin et al. (2012). In brief, a large Cs^+ primary beam of ~250 pA current with an accelerating voltage of 16 kV was rastered on the sample surface over a 12 µm × 12 µm area during a 3 min pre-sputter to eliminate any remaining surface contamination. Secondary ions of ^1H, ^2H, ^{12}C, and ^{18}O were then collected simultaneously, from the central 5 µm × 5 µm area of a 10 µm × 10 µm raster, on electron multipliers for ~20 min. An electron gun was used for charge compensation. The mass resolving power was set to ~4000, more than sufficient to resolve $^2H^+$ from H_2^+. OH contents were calibrated using the measured $^1H/^{18}O$ ratio and the calibrations derived using reference apatites with known OH contents, which were also used to correct the measured D/H ratios for instrumental mass fractionation (details are given in Tartèse et al., 2013). Apatite OH contents and D/H ratios, given using standard delta (δ) notation with respect to the D/H ratio of the Vienna standard mean

ocean water (VSMOW), are reported with their 2σ uncertainties, derived from the reproducibility of associated sets of standard analyses and the internal precision of each analysis, in Table DR2. The readers interested in the potential issue of terrestrial contamination, especially for lunar meteorites, should refer to the detailed discussion provided by Tartèse et al. (2013). Secondary ion images of ^{1}H, ^{13}C, ^{18}O, and ^{19}F were collected over a 30 μm × 30 μm area enclosing a glass + melt inclusion + apatite assemblage in lunar sample 15386. Five planes of image data, divided in 256 × 256 pixels, were collected using a dwell time of 0.5 ms/pixel, representing an acquisition time of ~3 min, and were then combined, aligned, and processed using the L'image software (Larry Nittler, Carnegie Institute of Washington, USA; http://home.dtm.ciw.edu/users/nittler/limage_manual.pdf).

ACKNOWLEDGMENTS

We thank the NASA Curation and Analysis Planning Team for Extraterrestrial Materials (CAPTEM) for allocation of Apollo Mission samples, and the Natural History Museum, London, for allocation of lunar meteorite NWA 773 polished sections. Michael Roden, Jeff Taylor, and an anonymous reviewer are thanked for their comments and suggestions. This research was supported by a Science and Technology Facilities Council (STFC) research grant to Anand (grant ST/I001298/1) and a NASA Lunar Advanced Science for Exploration Research grant to McCubbin (grant NNX13AK32G). We acknowledge the UK Cosmochemical Analysis Network (UKCAN) (grant ST/I001964/1 to Franchi) for NanoSIMS machine time allocation.

REFERENCES CITED

Alexander, C.M.O'D., Bowden, R., Fogel, M.L., Howard, K.T., Herd, C.D.K., and Nittler, L.R., 2012, The provenances of asteroids, and their contributions to the volatile inventories of the terrestrial planets: Science, v. 337, p. 721–723, doi:10.1126/science.1223474.

Barnes, J.J., Franchi, I.A., Anand, M., Tartèse, R., Starkey, N.A., Koike, M., Sano, Y., and Russell, S.S., 2013, Accurate and precise measurements of the D/H ratio and hydroxyl content in lunar apatites using NanoSIMS: Chemical Geology, v. 337–338, p. 48–55, doi:10.1016/j.chemgeo.2012.11.015.

Barnes, J.J., Tartèse, R., Anand, M., McCubbin, F.M., Franchi, I.A., Starkey, N.A., and Russell, S.S., 2014, The origin of water in the primitive Moon as revealed by the lunar highlands samples: Earth and Planetary Science Letters, v. 390, p. 244–252, doi:10.1016/j.epsl.2014.01.015.

Boyce, J.W., and Hervig, R.L., 2008, Magmatic degassing histories from apatite volatile stratigraphy: Geology, v. 36, p. 63–66, doi:10.1130/G24184A.1.

Boyce, J.W., Liu, Y., Rossman, G.R., Guan, Y., Eiler, J.M., Stolper, E.M., and Taylor, L.A., 2010, Lunar apatite with terrestrial volatile abundances: Nature, v. 466, p. 466–469, doi:10.1038/nature09274.

Esat, T.M., 1988, Physicochemical isotope anomalies: Geochimica et Cosmochimica Acta, v. 52, p. 1409–1424, doi:10.1016/0016-7037(88)90211-6.

Greenwood, J.P., Itoh, S., Sakamoto, N., Warren, P., Taylor, L., and Yurimoto, H., 2011, Hydrogen isotope ratios in lunar rocks indicate delivery of cometary water to the Moon: Nature Geoscience, v. 4, p. 79–82, doi:10.1038/ngeo1050.

Harrison, T.M., and Watson, E.B., 1984, The behaviour of apatite during crustal anatexis: Equilibrium and kinetic considerations: Geochimica et Cosmochimica Acta, v. 48, p. 1467–1477, doi:10.1016/0016-7037(84)90403-4.

Hauri, E.H., Weinreich, T., Saal, A.E., Rutherford, M.C., and Van Orman, J.A., 2011, High pre-eruptive water contents preserved in lunar melt inclusions: Science, v. 333, p. 213–215, doi:10.1126/science.1204626.

Hui, H., Peslier, A.H., Zhang, Y., and Neal, C.R., 2013, Water in lunar anorthosites and evidence for a wet early Moon: Nature Geoscience, v. 6, p. 177–180, doi:10.1038/ngeo1735.

Lécuyer, C., Gillet, P., and Robert, F., 1998, The hydrogen isotope composition of seawater and the global water cycle: Chemical Geology, v. 145, p. 249–261, doi:10.1016/S0009-2541(97)00146-0.

Mathez, E.A., and Webster, J.D., 2005, Partitioning behavior of chlorine and fluorine in the system apatite–silicate melt–fluid: Geochimica et Cosmochimica Acta, v. 69, p. 1275–1286, doi:10.1016/j.gca.2004.08.035.

McCubbin, F.M., Steele, A., Nekvasil, H., Schnieders, A., Rose, T., Fries, M., Carpenter, P.K., and Jolliff, B.L., 2010a, Detection of structurally bound hydroxyl in fluorapatite from Apollo mare basalt 15058,128 using TOF-SIMS: The American Mineralogist, v. 95, p. 1141–1150, doi:10.2138/am.2010.3448.

McCubbin, F.M., Steele, A., Hauri, E.H., Nekvasil, H., Yamashita, S., and Hemley, R., 2010b, Nominally hydrous magmatism on the Moon: Proceedings of the National Academy of Sciences of the United States of America, v. 107, p. 11,223–11,228, doi:10.1073/pnas.1006677107.

McCubbin, F.M., Jolliff, B.J., Nekvasil, H., Carpenter, P.K., Zeigler, R.A., Steele, A., Elardo, S.M., and Lindsley, D.H., 2011, Fluorine and chlorine abundances in lunar apatite: Implications for heterogeneous distributions of magmatic volatiles in the lunar interior: Geochimica et Cosmochimica Acta, v. 75, p. 5073–5093, doi:10.1016/j.gca.2011.06.017.

McCubbin, F.M., Hauri, E.H., Elardo, S.M., Vander Kaaden, K.E., Wang, J., and Shearer, C.K., 2012, Hydrous melting of the martian mantle produced both enriched and depleted shergottites: Geology, v. 40, p. 683–686, doi:10.1130/G33242.1.

McCubbin, F.M., Elardo, S.M., Shearer, C.K., Smirnov, A., Hauri, E.H., and Draper, D.S., 2013, A petrogenetic model for the comagmatic origin of chassignites and nakhlites: Inferences from chlorine-rich minerals, petrology, and geochemistry: Meteoritics and Planetary Science, v. 48, p. 819–853, doi:10.1111/maps.12095.

Saal, A.E., Hauri, E.H., Langmuir, C.H., and Perfit, M.R., 2002, Vapour undersaturation in primitive mid-ocean-ridge basalt and the volatile content of Earth's upper mantle: Nature, v. 419, p. 451–455, doi:10.1038/nature01073.

Saal, A.E., Hauri, E.H., Lo Cascio, M., Van Orman, J.A., Rutherford, M.C., and Cooper, R.F., 2008, Volatile content of lunar volcanic glasses and the presence of water in the Moon's interior: Nature, v. 454, p. 192–195, doi:10.1038/nature07047.

Saal, A.E., Hauri, E.H., Van Orman, J.A., and Rutherford, M.J., 2013, Hydrogen isotopes in lunar volcanic glasses and melt inclusions reveal a carbonaceous chondrite heritage: Science, v. 340, p. 1317–1320, doi:10.1126/science.1235142.

Sha, L.K., 2000, Whitlockite solubility in silicate melts: Some insights into lunar and planetary evolution: Geochimica et Cosmochimica Acta, v. 64, p. 3217–3236, doi:10.1016/S0016-7037(00)00420-8.

Sharp, Z.D., McCubbin, F.M., and Shearer, C.K., 2013, A hydrogen-based oxidation mechanism relevant to planetary formation: Earth and Planetary Science Letters, v. 380, p. 88–97, doi:10.1016/j.epsl.2013.08.015.

Tartèse, R., and Anand, M., 2013, Late delivery of chondritic hydrogen into the lunar mantle: Insights from mare basalts: Earth and Planetary Science Letters, v. 361, p. 480–486, doi:10.1016/j.epsl.2012.11.015.

Tartèse, R., Anand, M., Barnes, J.J., Starkey, N.A., Franchi, I.A., and Sano, Y., 2013, The abundance, distribution, and isotopic composition of Hydrogen in the Moon as revealed by basaltic lunar samples: Implications for the volatile inventory of the Moon: Geochimica et Cosmochimica Acta, v. 122, p. 58–74, doi:10.1016/j.gca.2013.08.014.

Taylor, G.J., Martel, L.M.V., and Spudis, P.D., 2012, The Hadley-Apennine KREEP basalt igneous province: Meteoritics and Planetary Science, v. 47, p. 861–879, doi:10.1111/j.1945-5100.2012.01364.x.

Vander Kaaden, K.E., McCubbin, F.M., Whitson, E.S., Hauri, E.H., and Wang, J., 2012, Partitioning of F, Cl, and H_2O between apatite and a synthetic shergottite liquid (QUE 94201) at 1.0 GPa and 990–1000°C: Houston, Texas, Lunar and Planetary Institute, Lunar and Planetary Science Conference XLIII, Abstract 1247.

Wang, Y., Guan, Y., Hsu, W., and Eiler, J.M., 2012, Water content, chlorine and hydrogen isotope compositions of lunar apatite: Cairns, Australia, Lunar and Planetary Institute, Annual Meteoritical Society Meeting LXXV, Abstract 5170.

Manuscript received 11 November 2013
Revised manuscript received 3 February 2014
Manuscript accepted 5 February 2014

Printed in USA